J. Math. Biol. (2008) 56:827–839
DOI 10.1007/s00285-007-0140-4

Mathematical Biology

Seasonal dynamics and thresholds governing recurrent epidemics

Ronen Olinky · Amit Huppert · Lewi Stone

Received: 11 June 2007 / Revised: 12 October 2007 / Published online: 8 November 2007

Abstract Driven by seasonality, many common recurrent infectious diseases are characterized by strong annual, biennial and sometimes irregular oscillations in the absence of vaccination programs. Using the seasonally forced SIR epidemic model, we are able to provide new insights into the dynamics of recurrent diseases and, in some cases, specific predictions about individual outbreaks. The analysis reveals a new threshold effect that gives clear conditions for the triggering of future disease outbreaks or their absence. The threshold depends critically on the susceptibility S_0 of the population after an outbreak. We show that in the presence of seasonality, forecasts based on the susceptibility S_0 are more reliable than those based on the classical reproductive number R_0 from the conventional theory.

Keywords Seasonally forced model · R_0 · SIR · Threshold · Epidemic · Chaos

Mathematics Subject Classification (2000) Nonlinear dynamics · Mathematical epidemiology

1 Introduction

Mathematical models of infectious diseases have contributed greatly to our understanding of the dynamics of epidemics as they spread through large populations [1–13]. Here we are principally interested in modelling recurrent epidemics, best exemplified

R. Olinky · A. Huppert · L. Stone (✉)
Biomathematics Unit, Faculty of Life Sciences, Tel Aviv University, Ramat Aviv 69978, Israel
e-mail: lewi@post.tau.ac.il

A. Huppert
Center for Risk Analysis, Gertner Institute, Sheba Medical Center, Tel Hashomer 52621, Israel

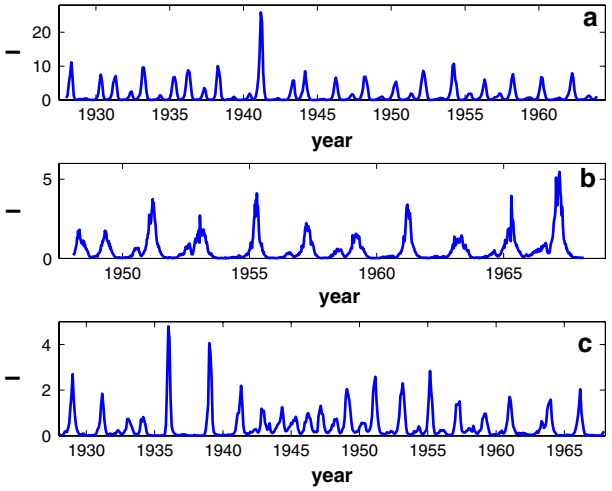

Fig. 1 Time series of reported measles infective cases (in thousands) from the largest cities in the US, UK and Denmark in the pre-vaccination era. Data obtained from Ref. [2] and http://www.zoo.ufl.edu/bolker/

by childhood infectious diseases such as measles, mumps, whooping cough and chickenpox, but also includes influenza, hepatitis, syphilis and many other high impact diseases. Figure 1 shows three classical time series of reported cases of measles in the United States (New York), the United Kingdom (London) and Denmark (Copenhagen) in the pre-vaccination era. Major epidemics usually peak close to spring each year and on many occasions every second year when the dynamics are biennial. However, there is also a strong erratic and possibly chaotic component [5–7,9,11,14] as seen in the variability of epidemic intensity, and in the intermittent jumps between periods of annual and biennial dynamics.

It is now well understood that seasonality is often the primary factor responsible for recurrent epidemic cycles. In the case of childhood infectious diseases, in which infection is transmitted through contact, the seasonality is overtly apparent upon visualising the average contact rate between individuals as it changes over the year [2,7]. The number of contacts peak most strongly in winter reflecting the high disease transmission rates amongst children which initiates at the beginning of the school term. The complex disease oscillations that emerge are an outcome of the interaction between the externally imposed annual seasonality as expressed in the contact rate and the intrinsic oscillatory dynamics of the disease itself. It thus becomes natural to model these diseases as periodically forced nonlinear systems [3,4,6,8,9].

The following analysis is based on the classical forced 'SIR' epidemic model. Despite many efforts over the last decades, it has been difficult to gain general quantitative or analytical insights into the operation of this model [9–13]. This is an outcome of the complex synchronization effects that can evolve between the external forcing and the natural oscillations of the nonlinear model [14]. The analysis advanced here attempts to make progress in this direction by focusing on what we term "skipping" dynamics. As the measles time series in Fig. 1 make evident, there are a significant number of years in which major epidemics do not appear to trigger at all, i.e., they "skip."

Figure 2 indicate that these skipping events are also intrinsic to the forced SIR model when parameterised in the chaotic regime. In fact, it is difficult if not impossible to locate realistic chaotic parameter regimes in which outbreaks occur regularly each year. This contrasts with the well known Rossler oscillator, and several ecological foodweb models whose outbreaks recur regularly but whose amplitude vary chaotically in time (i.e., the Uniform Phase Chaotic Amplitude oscillations discussed in [15]). The goal of the present paper is to develop a "language of skips" that makes it possible to predict under what conditions the next outbreak is likely to occur, and how many "skips" might be expected after any given outbreak.

The paper is organised as follows. We first give basic details describing the standard SIR model under conditions of forcing and very briefly overview its dynamics via phase plane analysis. The model's dynamics are categorized and studied in two different regimes—the fast outbreak dynamics and the slow susceptible build up regime where skips occur. In approximating the latter, threshold conditions are derived that determine the presence or absence of skips in the years ahead. We then provide an intuitive interpretation explaining the threshold result and relate this to the better known predictor, the reproductive number R_0. Finally we discuss how predictions based on the conventional reproductive number R_0 may be misleading in systems driven by seasonality.

2 The seasonally forced SIR model

In the traditional SIR model [1], each member of the population is considered to belong to one of three classes: Susceptible individuals (S), Infected individuals (I), and Removed individuals (R). Each individual begins in the susceptible class S, only to move to the infected class I after coming into contact with an infected person. Infected individuals eventually recover from the disease and then move on to the recovered class R. Being "recovered" and unable to be infected once again, they are essentially removed from the population and play no further role in the dynamics. Epidemics are continuously fueled by the constant supply of new susceptibles that arise due to the birth of new individuals.

The SIR model with vital rates (birth and death) takes the following form:

$$\begin{aligned} \dot{S} &= \mu N - \mu S - \beta(t) SI/N, \\ \dot{I} &= \beta SI/N - \gamma I - \mu I, \\ \dot{R} &= \gamma I - \mu R. \end{aligned} \tag{1}$$

All classes of the population reproduce and die at the same per-capita rate μ, so that an average lifetime is $1/\mu$ years. The parameter γ represents the rate at which infected individuals recover giving mean infection time $1/\gamma$ years. In practice $\mu \ll \gamma$. For homogeneously mixing populations, the rate of contact between S and I individuals is proportional to the product SI, (the Law of Mass Action). Note that the total population size $S + I + R = N$ is constant ($\forall t,\ \dot{S} + \dot{I} + \dot{R} = 0$), and it is only necessary to work with the first two equations in Eq. (1). By convention, we set $N = 1$, and S, I, and R are proportions of the entire population.

As mentioned, for childhood infectious diseases the contact rate ($\beta(t)$) is seasonal and peaks strongly in winter reflecting the beginning of the school term. A commonly used scheme takes $\beta(t) = \beta_0(1 + \delta \sin(2\pi t))$ where β_0 gives the mean contact rate, $0 < \delta < 1$ represents the strength of the seasonal forcing, and t has units of years. However, to help simplify the analysis, we initially make the approximation (see [9]) that there are only two seasons each year as follows:

$$\beta(t) = \begin{cases} \beta^+ = \beta_0(1+\delta) & \text{High season} \\ \beta^- = \beta_0(1-\delta) & \text{Low season} \end{cases} \tag{2}$$

Over time the seasons change sequentially $High \rightarrow Low \rightarrow High \rightarrow \cdot$. The Low season begins at times $t_n, n = 0, 2, 4, \ldots$, with a low contact rate β^- and lasts for a time interval $p * \tau = T^-$, where τ is the period length (i.e., a year) and $0 < p < 1$. This is followed by the High season at times $t_n, \quad n = 1, 3, 5, \ldots$, with high contact rate β^+, and lasts for $(1 - p) * \tau = T^+$. We proceed to characterize the model dynamics by developing maps that track the numbers of susceptibles and infectives between seasons. Elements of this approach may be found in the work of [16–19], although without the full accounting that is attempted here.

In simulations, we follow [12,20] and incorporate a small amount of immigration on a continuous basis. The immigration helps reduce the population variability generated by the forced model, especially the unrealistically large "peaks and valleys" that span many orders of magnitude in the infective numbers during and between epidemics. This is achieved by rewriting the mass action term SI in Eqs. (1) as $S(I + \epsilon)$ where the small immigration term is $\epsilon = 10^{-12}$ in the simulation of Fig. 2a. Other immigrations schemes have been tested and yield similar results. In fact, all theoretical results reported here have no dependence on the presence or absence of immigration.

For weak forcing (δ), the model is characterized by small amplitude solutions of period-1 annual oscillations [9]. As the forcing is increased, the solution bifurcates to period-2 (biennial oscillations) where the model generates an epidemic every second year and a "skip" every other year in which the outbreak is suppressed. As δ is increased further the familiar period-doubling route to chaos is observed [4,8].

The chaotic regime of the model has a strong tendency to "skip" for periods of several consecutive years (see Fig. 2a, c).

Figures 2b, d and 3 show trajectories of the seasonally forced model (Eqs. 1) as they rotate counter-clockwise around the $S - w$ phase-plane ($w = \log I$) when the dynamics are chaotic and biennial respectively. As the seasons change, the trajectory is attracted to the quasi-equilibrium associated with each season. Non-equilibrium behaviour arises as the trajectory is attracted to each quasi-equilibrium but kicked away before ever reaching it. The trajectory is thus kicked away from one quasi-equilibrium to the next. Figure 3 shows biennial behaviour with a large outbreak in the upper portion of the phase plane (**UPP**) in the first year, followed by a "skip" in the lower portion of phase plane (**LPP**) in the second year. The trajectory is kicked between the two equilibria marked as circles. The S nullcline (where $dS/dt = 0$) divides the phase-plane into its two regimes, the UPP and LPP. For realistic parameters, each regime is characterized by its own specific time scale.

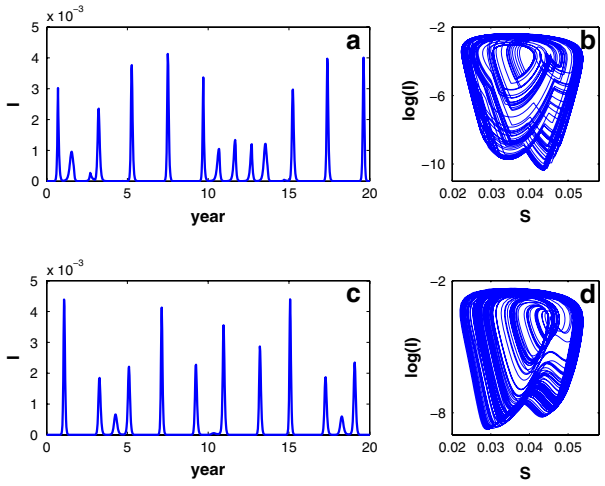

Fig. 2 **a, b** Time series and phaseplane diagram of a chaotic simulation of the forced SIR model with parameters: $\mu = 0.02$, $\gamma = 66$, $\beta_0 = 1600$, $\delta = 0.18$, $\epsilon = 10^{-12}$ High season = 0.5 year; Low season = 0.5 year. **c, d** Time series and phaseplane diagram of a chaotic simulation of the forced SIR model with *sinusoidal forcing* parameters: $\mu = 0.016$, $\gamma = 66$, $\beta_0 = 1590$, $\delta = 0.2$, $\epsilon = 0.12 \times 10^{-9}$

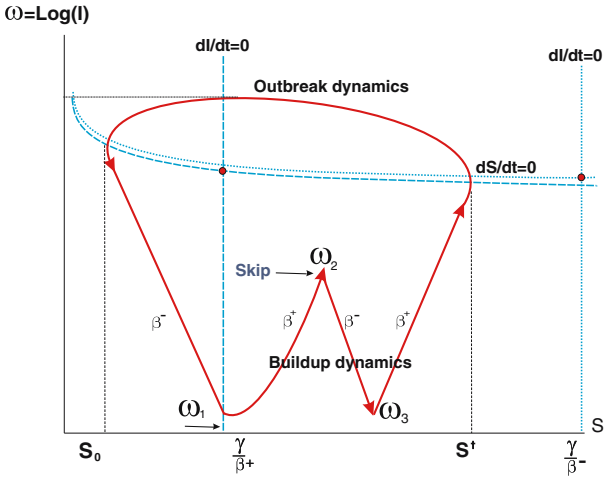

Fig. 3 Phase plane diagram for a biennial cycle with infectives ($w = \log I$) plotted as a function of susceptible numbers (S). The SIR model's (1) trajectory rotates counter-clockwise around the phase plane. The trajectory is attracted to the quasi-equilibrium associated with each season (the null-cline intersection, *circles*). As the season (and contact-rates $\beta^{\pm}$) change, the trajectory is kicked away from one equilibrium to the next

I. Fast Epidemic Dynamics: When a major epidemic is in progress the mortality and birth rate terms μ in (1) are relatively small and have little influence on the dynamics. The outbreak takes place in the UPP seen in Fig. 3. Thus when $I \gg \frac{\mu}{S\beta^{\pm}}$ (above the S null-cline $dS/dt = 0$) it is possible to approximate Eqs. (1) as

$$\dot{S} = -\beta(t)SI, \quad \dot{I} = I(\beta(t)S - \gamma - \mu). \tag{3}$$

For a given value of β (i.e., over a single season) it is possible to approximate $S(t)$, $I(t)$ and $R(t)$ analytically (see, e.g., [22,23]) if the initial conditions are known in advance.

II. Slow buildup dynamics: During a major epidemic, the number of infectives drop rapidly. In the phase-plane (Fig. 3), when $I \ll \frac{\mu}{S\beta^{\pm}}$ and the trajectory has fallen below the S null-cline (i.e., in the LPP), then Eq. (1) may be approximated as

$$\dot{S} = \mu, \quad \dot{I} = I(\beta(t)S - \gamma - \mu), \tag{4}$$

where (S_0, I_0) are initial conditions. Note that in the susceptible buildup regime the rate of change of S is solely due to new births and is slow compared to the very fast changes experienced during an outbreak. Therefore, the system spends most of its time in the LPP. It is useful to set S_0 as the minimum value of susceptibles reached in the wake of an epidemic (see Fig. 3). We show that this new epidemiological parameter is of great importance.

3 Enumerating the number of skips as a function of S_0

A skip is the absence of an outbreak that would normally be expected in the High Season. Skips necessarily occur in the LPP (Fig. 3), and are governed by approximating Eqs. (4) which we proceed to study further. Each year is taken to have only two seasons. It begins in the Low season at times t_n, $n = 0, 2, 4, \ldots$, with a low contact rate $\beta^- = \beta_0(1 - \delta)$ and lasts for a time interval $p * \tau = T^-$, where τ is the period length (i.e., a year) and $0 < p < 1$. This is followed by the High season at times t_n, $n = 1, 3, 5, \ldots$, with high contact rate $\beta^+ = \beta_0(1 + \delta)$, which lasts for $(1 - p) * \tau = T^+$.

The overall strategy for solving system (4) is to calculate the solution in the time intervals between t_n and t_{n+1}. Each time interval will have a constant contact rate (i.e., either β^+ or β^-) and initial values S_n and I_n. The scheme stops whenever $I_n \geq \frac{\mu}{\beta S_n}$ which is the S null-cline curve in the (S, I) phase plane. At this point we return back to the outbreak solutions generated by Eqs. (3).

The sharp points where the infected population reach the local maxima I_n lying below the S null-cline are defined as skipping points (see Fig. 3). These maxima arise because the trajectory is curtailed in the phase plane whenever there is a change of season, and is prevented from continuing on to form a large amplitude epidemic.

The difference between a skipping point and an epidemic peak is not just a question of magnitude. During a skip the susceptible population **always** continues to increase despite the fact that the number of infectious individuals pass through a maximum. In contrast, during a major epidemic, the susceptible population declines. This provides a natural topological criterion to distinguish "skips" from outbreaks.

To simplify the analysis the model variables are rescaled as follows:

$$s = \frac{\beta_0}{\gamma + \mu} S, \quad w = \log I, \quad m = \frac{\beta_0 \mu}{\gamma + \mu}, \quad \text{and} \quad \Gamma = \gamma + \mu. \tag{5}$$

An equivalent system to (4) is

$$\dot{s} = m, \quad \frac{\dot{w}}{\Gamma} = (1 \pm \delta)s - 1. \tag{6}$$

Observe that the susceptibles increase linearly with a constant rate m:

$$s(t) = mt + c_0 \tag{7}$$

where $c_0 = s_0 - mt_0$. From the phase plane (Fig. 3) define (s_1, w_1) as the coordinates of the sharp skipping point that results from the change of $\beta(t)$ as it jumps from β^- to β^+. All sharp points (s_n, w_n) are produced by this mechanism. By integrating system (6) between two neighboring sharp points and assuming that t_0 occurs during the low season ($\beta(t) = \beta^-$) we obtain

$$\frac{w_1 - w_0}{\Gamma} = (1 - \delta) \int_{t_o}^{T^-} (mt + c_0)dt - T^- + t_0. \tag{8}$$

The analytic manipulation is more transparent when the forcing function is taken to be symmetric, $T^- = T^+ = T$. In this case:

$$\frac{w_1 - w_0}{\Gamma} = (1 - \delta)\frac{mT^2}{2} + T[c_0(1 - \delta) - 1] - c_1 \tag{9}$$

where $c_1 = (1 - \delta)\frac{mt_0^2}{2} + t_0[c_0(1 - \delta) - 1]$. For general $n > 0$ we obtain

$$\frac{w_{n+1} - w_n}{\Gamma} = (1 - (-1)^n\delta) \int_{nT}^{(n+1)T} (mt + c_0)dt - T, \tag{10}$$

and thus

$$\frac{w_{n+1} - w_n}{\Gamma} = (1 - (-1)^n\delta)\left[\frac{mT^2}{2}(2n + 1)\right] + T[c_0(1 - (-1)^n\delta) - 1]. \tag{11}$$

The w_n may now be written in recursive form to ultimately obtain

$$\frac{w_n}{\Gamma} = \frac{w_0}{\Gamma} - c_1 + \frac{m}{2}T^2[n^2 + (-1)^n n\delta] + T\left[n(c_0 - 1) + \frac{(-1)^n - 1}{2}\delta c_0\right]. \tag{12}$$

To simplify the analysis, it is reasonable to make the approximation $t_0 = 0$, resulting in $c_1 = 0$, and $c_0 = s_0$. Since the forcing period is taken to be $\tau = 2T = 1$year, the formula for w_n may be rewritten as

$$w_n - w_0 = \frac{\Gamma}{8}(mn^2\tau^2 + ((-1)^n m\delta\tau^2 + 4[s_0 - 1]\tau)n + 2((-1)^n - 1)\delta s_0\tau). \tag{13}$$

Thus the sharp points w_n, for even and odd n, follow two parabolas in the phase plane, and effectively envelope the dynamics of the forced model. The trajectory moves from one parabola to the other with every change of season.

After a major epidemic the trajectory is seen to shadow the w_n first dropping down the (s, w) phase plane, only to later rise while susceptibles build up to fuel the next outbreak. Note that as susceptibles increase linearly in time (see Eq. (7)) in the LPP, then plotting w_n against either s or time (n) yields the same parabola.

As observed in Fig. 3, the s null-cline ($I \ll \frac{\mu}{s\beta^{\pm}}$) in the phase plane in the vicinity of the attractor can be approximated as a reasonable horizontal line for realistic parameters. (This is because infectives decrease exponentially by several orders of magnitude as the trajectory circuits the LPP while s changes linearly.) Thus this recursive scheme stops whenever $w_n > \log(\frac{m}{s\beta^{\pm}}) \approx w_0$. Let us define $\hat{n} \approx 2(k+1)$ to be the smallest n where $w_n > \log(\frac{m}{s\beta^{\pm}}) \approx w_0$. Then the overall number of skips is given by $k \approx [\frac{\hat{n}}{2}] - 1$ where $[x]$ is the integer value of x. From 13 it follows that we look for the smallest even value of n that fulfills:

$$m\hat{n}^2 + m\delta\hat{n} + 4(s_0 - 1)\hat{n}/\tau > 0, \tag{14}$$

or

$$\hat{n} > \frac{4}{m\tau}(1 - s_0) - \delta. \tag{15}$$

Recalling that $\hat{n} \approx 2(k+1)$ then the threshold can be calculated in terms of s_0 as

$$s_0 > 1 - \frac{m(k+1)\tau}{2} - \frac{\delta m\tau}{4}. \tag{16}$$

Changing back to the natural variables (5) we arrive at

$$S_c(k) = \frac{\gamma + \mu}{\beta_0} - \frac{\mu(k+1)\tau}{2} - \frac{\delta\mu\tau}{4}. \tag{17}$$

where again the forcing period is $\tau = 1 - \text{year}$. Then $S_c(k)$ acts as a threshold such that:

- if $S_0 > S_c(k)$ the trajectory must continue on to have less than or equal to k consecutive skips in the coming years.
- if $S_0 < S_c(k)$, the trajectory must be greater than k consecutive skips in the coming years.

For the important case of $k = 0$, let $S_c = S_c(0)$ giving the threshold condition:

- if $S_0 > S_c(0)$ there is an outbreak in the following year (i.e., zero skips).
- if $S_0 < S_c(0)$, the trajectory must have at least one or more consecutive skips in the coming years.

4 Testing the threshold and its robustness

The effectiveness of the threshold prediction may be demonstrated through the study of simulated epidemic time series. By integrating the forced SIR model in the chaotic regime it was possible to generate time series with skips and variability similar to real world data. That is, where the epidemics are erratic and may skip unpredictably from one year to the next as seen in the time series of Fig. 1. The main advantage of the chaotic time series lies not in their (possibly controversial) realism, but in their variability—a feature which facilitates checking the legitimacy of the above threshold point S_c.

Figure 4 shows explicitly how the parameter S_0, which characterizes population susceptibility, gives accurate predictions of future outbreaks. In Fig. 4a (inset), the time τ between two successive large-scale epidemics A and B, is plotted as a function of the minimum number of susceptibles S_0 left in the wake of the first outbreak A. For the given model parameters (Fig. 4 legend), the theoretical critical susceptible threshold

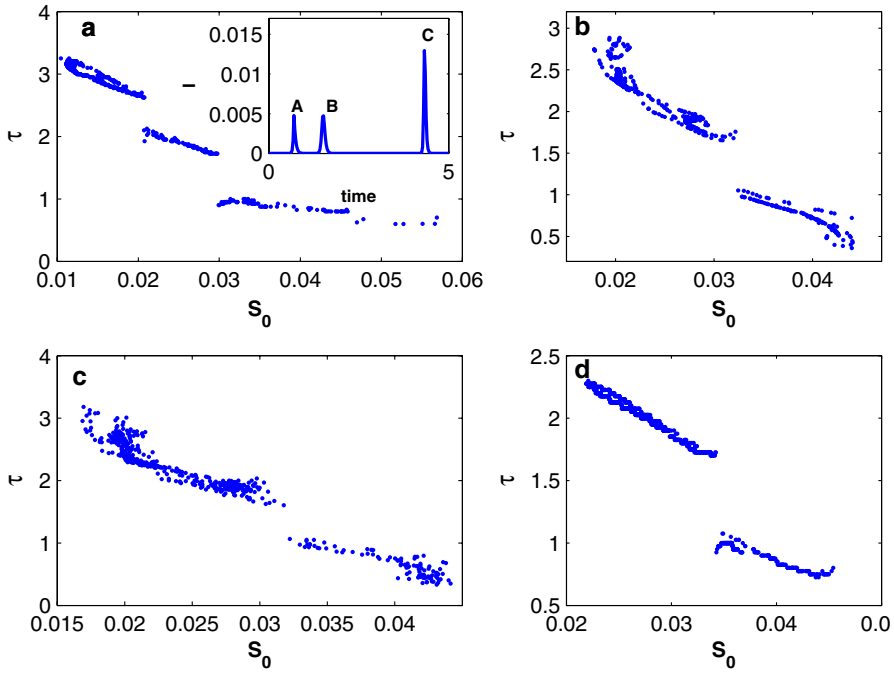

Fig. 4 Testing the threshold prediction equation (17). **a** The forced SIR epidemic model (1) using the forcing of (2) was integrated in the chaotic regime to generate simulated time series of infectives (see inset) and susceptibles. The time τ between two successive large-scale epidemics. (e.g., A and B) plotted as a function of the susceptibles S_0 left in the wake of the previous epidemic (parameters for the simulated chaotic regime: $\mu = 0.02$, $\gamma = 66$, $\beta_0 = 1600$, $\delta = 0.34$; Forcing with High and Low seasons both $=$ 0.5 years). **b** As in **a** but with parameters as in Fig. 2a, **c** parameters as in **b but** the onset of Hi and Lo season varies randomly (uniformly) by up to ±10% and also the mean β_0 of the seasonal forcing varies randomly (uniformly) also by up to ±10% at each time step. **d** The same threshold but using sinusoidal forcing. Parameters as in Fig. 2c

($S_c(0) = 0.030$ from Eq. (17)) corresponds to the critical susceptible numbers seen in Fig. 4 that separates the annual dynamics ($\tau \approx 1$) from the biennial dynamics ($\tau \approx 2$) having a single skip. Also according to Eq. (17), $S_c(1) = 0.020$, corresponding to the critical number of susceptibles required to generate two consecutive skips.

The threshold is robust to changes in the form of the seasonal forcing $\beta(t)$. This can be seen in Fig. 4d which displays the same threshold effects but taking sinusoidal forcing $\beta(t) = \beta_0(1+\delta\sin(2\pi t))$. For the given parameters (Fig. 4 legend) the critical susceptible numbers as determined by Eq. (17) is $S_c = 0.033$, which sits very close to the threshold level seen in the simulation results of Fig. 4. The same threshold can be observed when more complicated term-time forcing (see [9]) is used (details available upon request). Moreover, we have investigated the influence of noise perturbations to the seasonal forcing term in several different ways and have found the results unusually robust even for relatively high intensity perturbations (see Fig. 4c for details).

5 Intuitive interpretation of threshold

Further insights regarding the formula for the threshold and the number of skips can be gained by analysing the model in the lower portion of the phase plane in the absence of forcing. Scaled equations (6) with $\delta = 0$ in the susceptible buildup regime, has as solutions

$$s(t) = mt + s_0, \quad w(t) = \Gamma t(mt/2 + s_0 - 1) + w_0. \tag{18}$$

Again, the (log) infectives, $w(t)$, follow a parabolic trajectory with time. To find the model's recovery time (t_r) between epidemics we seek the value of t where $w(t)$ returns to its initial value w_0 i.e., where $w(t) = w_0$, and must occur when $W(t) = t(mt/2 + s_0 - 1) = 0$ (cf. Eq. (14) taking $t = 2n$). Now $W(t) = 0$ has roots at $t_0 = 0$ and $t_1 = 2(1-s_0)/m$. Thus the model's recovery time between epidemics is approximated as $t_r = 2(1 - s_0)/m$ years. The number of skips is $k = [t_r] - 1 = [2(1 - s_0)/m] - 1$ which gives $s_0 = 1 - m(k+1)/2$. Changing back to the natural variables (5) we arrive at:

$$S_c(k) = \frac{\gamma + \mu}{\beta_0} - \frac{(k+1)\mu}{2}. \tag{19}$$

This criterion equation (19) (note the similarity to Eq. (17)) may be understood as follows. Firstly, consider the proportion of available susceptibles S' in the population precisely at the turning point of the parabola in the phase plane (see Fig. 5). S' must equal the initial amount of suseptibles S_0 at time t_0 plus the additional new susceptibles created from the birth process since time t_0. Since μ new suspectibles are created each year, having k skips requires

$$S' = S_0 + (k+1)\mu/2. \tag{20}$$

Define

$$R_0 = \frac{\beta_0 S}{\gamma + \mu} \tag{21}$$

where here β_0 is the contact rate averaged over a year. Although not the exact epidemiological reproduction number [1,23], it is apparent that R_0 may be viewed as the

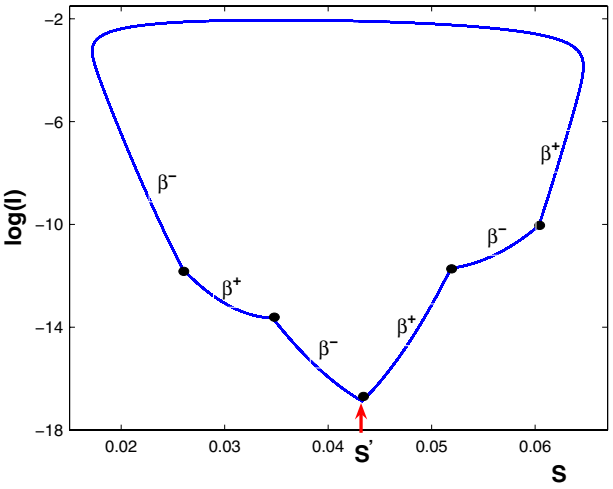

Fig. 5 A simulation of the forced model in the periodic regime (parameters used in the simulation: $\mu = 0.018$, $\gamma = 66$, $\beta_0 = 1600$, $\delta = 0.18$, $\epsilon = 0$). One sees how $w(t) = \log(I)$ descends in the phase plane reaching a minimum at $S' = 0.0433$ (marked by *arrow*). This value is approximately as predicted by Eq. (20) $S' = 0.0413$ for the unforced model according to the parameters used in the simulation. The *solid circles* sitting on the model trajectory indicate those points in time when the season changes

average number of secondary infections produced by a single infective individual in a population having a proportion of S susceptibles.

Equations (18) and (19) reveal that $S' = (\gamma + \mu)/\beta_0$ when $S_0 = S_c(k)$, so that $R_0 = 1$ when $S = S'$. Thus we see that the tendency of the w_n to reduce in the phase plane changes to a tendency of increase at the point where $R_0 = 1$, that is, where the average number of secondary infections is equal unity. Figure 5 displays a periodic orbit of the forced model where the turning point occurs very close to the prediction $S' = (\beta + \mu)/\gamma = 0.0413$. For the forced model, the reproductive number R_0 acts as a control on the trajectories rotation around the phase plane. The above reasoning clarifies how the epidemiological parameter S_0, which is a proxy for population susceptibility in the wake of a large epidemic, allows prediction of the occurrence or the inhibition of future epidemics.

6 Discussion

The simplified two-season forced model gives new insights that help explain the impact of seasonality in epidemiological systems. Perhaps the most important feature is the manner in which the transition from High to Low season often acts to curtail potential epidemics. This, in fact, is the mechanism that leads to skips—the sharp points in the LPP of Fig. 3. These sharp points are characterized by the initiation of an epidemic (infective numbers increasing), which is rapidly cut short (infectives decreasing) by the change to Low season. According to classical theory, increasing small numbers of infectives is suggestive that the reproductive number R_0 is greater than unit, a characteristic that is typically diagnosed as an epidemic scenario. Hence, this would

wrongly diagnoses skips induced by seasonality as large scale outbreaks. The classical predictions based on the reproductive number R_0 are thus misleading in the presence of seasonality. The threshold predictions of Eq. (17,19), however, appear to correctly predict whether a skip or epidemic will appear in the coming year.

The analysis demonstrates the importance of population susceptibility S_0 as measured after an outbreak and its usefulness in forecasting future epidemics or skips in the years ahead. The work goes beyond existing theories on the regular and irregular cycles of recurrent diseases in that it offers accurate epidemic predictions using a widely studied model otherwise considered analytically intractable. Moreover, because of the complex dynamics induced by seasonality, these predictions can differ from expectations obtained from the unforced model. The concepts presented here have particular relevance for seasonal diseases such as influenza A whose genetically based immunological properties drift in time, thereby continuously modifying the susceptibility of the host population [24,25]. In this case, the immunity of hosts depends on both previous exposure to the disease and immune memory. Hosts may be reinfected with the disease every few years due to evolutionary changes in the influenza viral antigens, with years of skips in between. The methods presented here provide a powerful technique for characterizing the dynamics of skips in diseases with antigenic evolution and/or host populations with waning immunity. Our results from this line of enquiry will shortly be reported.

Acknowledgments We gratefully acknowledge the support of the James S. McDonnell Foundation. We also thank the reviewers for their careful reading of our paper and for thoroughly checking all calculations.

References

1. Anderson, R.M., May, R.M.: Infectious Diseases of Humans: Dynamics and Control. Oxford University Press, New York (1991)
2. London, W.P., Yorke, J.A.: Recurrent outbreaks of measles, chickenpox and mumps. 1. Seasonal variation in contact rates. Am. J. Epidemiol. **98**, 453–468 (1973)
3. Stone, L., Olinky, R., Huppert, A.: Seasonal dynamics of recurrent epidemics. Nature **446**, 533–536 (2007)
4. Billings, L., Schwartz, I.B.: Exciting chaos with noise: unexpected dynamics in epidemic outbreaks. J. Math. Biol. **44**, 31–48 (2002)
5. Olsen, L.F., Truty, G.L., Schaffer, W.M.: A nonlinear dynamics analysis of childhood epidemics in Copenhagen, Denmark. Theor. Pop. Biol. **33**, 344–370 (1998)
6. Olsen, L.F., Schaffer, W.M.: Chaos versus noisy periodicity: alternative hypotheses for childhood epidemics. Science **249**, 499–504 (1990)
7. Fine, P.E.M., Clarkson, J.A.: Measles in England and Wales—I: an analysis of factors underlying seasonal patterns. Int. J. Epidemiol. **11**, 5–14 (1982)
8. Aron, J.L., Schwartz, I.B.: Seasonality and period-doubling bifurcations in an epidemic model. J. Theor. Biol. **110**, 665–679 (1984)
9. Keeling, M., Rohani, P., Grenfell, B.T.: Seasonally forced disease dynamics explored as switching between attractors. Physica D **148**, 317–335 (2001)
10. Schwartz, I.B., Smith, H.L.: Infinite subharmonic bifurcation in an SEIR epidemic model. J. Math. Biol. **18**, 233–253 (1983)
11. Earn, D.J.D., Rohani, P., Bolker, B.M., Grenfell, B.T.: A simple model for complex dynamical transitions in epidemics. Sci. **287**, 667–670 (2000)
12. Engbert, R., Drepper, F.R.: Chance and chaos in population biology—models of recurrent epidemics and food chain dynamics. Chaos Solitons Fractals **4**, 1147–1169 (1994)

13. Sugihara, G., May, R.M.: Nonlinear forecasting as a way of distinguishing chaos from measurement error in time-series. Nature **344**, 734–741 (1990)
14. Pikovsky, A., Rosenblum, M., Kurths, J.: Synchronization: A Universal Concept in Nonlinear Sciences. Cambridge University Press, Cambridge (2001)
15. Blasius, B., Huppert, A., Stone, L.: Complex dynamics and phase synchronization in spatially extended ecological systems. Nature **339**, 354–359 (1999)
16. Roberts, M.G., Heesterbeek, J.A.P.: A simple parasite model with complicated epidemics. J. Math. Biol. **37**, 272–290 (1998)
17. Roberts, M.G., Kao, R.R.: The dynamics of an infectious disease in a population with birth pulses. Math. Biosci. **149**, 23–26 (1998)
18. Andreasen, V., Frommelt, T.: A school-oriented, age-structured epidemic model. SIAM J. Appl. Math. **65**, 1870–1887 (2005)
19. Gog, J.R., Rimmelzwaan, G.F., Osterhaus, A.D.M.E., Grenfell, B.T.: Population dynamics of rapid fixation in cytotoxic T lymphocyte escape mutants of influenza A. PNAS **100**, 11143–11147 (2003)
20. Ferguson, N.M., May, R.M., Anderson, R.M.: Measles: persistence and synchronicity in disease dynamics. In: Tilman, D., Kareiva, P. (eds.) Spatial Ecology. Princeton University Press, pp. 137–157 (1997)
21. Schaffer, W.M., Kot, M.: Nearly one dimensional dynamics in an epidemic. J. Theor. Biol. **112**, 403–427 (1985)
22. Kermack, W.O., McKendrick, A.G.: Contributions to the mathematical theory of epidemics. Proc. Roy. Soc. A. **115**, 700–721 (1927)
23. Murray, J.D.: Mathematical Biology, 2edn. Springer, Berlin (1989)
24. Pease, C.M.: An evolutionary epidemiological mechanism, with applications to type A influenza. Theor. Pop. Biol. **31**, 422–452 (1987)
25. Andreasen, V.: Dynamics of annual influenza A epidemics with immuno-selection. J. Math. Biol. **46**, 504–536 (2003)